

Supporting Information

Microenvironment Control of Porphyrin Binding, Organization, and Function in Peptide Nanofiber Assemblies

Lee A. Solomon¹, Anna R. Wood¹, Matthew E. Sykes¹, Benjamin T. Diroll¹, Gary P. Wiederrecht¹, Richard D. Schaller^{1,2}, and H. Christopher Fry^{1*}.

¹Center for Nanoscale Materials, Argonne National Laboratory, Lemont, IL 60439 United States

²Department of Chemistry, Northwestern University, Evanston, IL 60208, United States

Supplemental Methods

Peptide Synthesis: Solid-phase peptide synthesis (SPPS) of c16-AHX₃K₃-CO₂H was carried out using standard Fmoc chemistry (CS Bio Co. automated peptide synthesizer, CS136XT) A preloaded resin, Fmoc-Lys(Boc)-Wang resin (0.25mmol synthetic scale, loading capacity: 0.77mmol/g, Chem Impex) was used as the solid support. A solution of 20% piperidine (Sigma-Aldrich) in dimethylformamide (Fisher Chemical, Bioreagent Grade) was used as the deprotecting reagent with subsequent 5 and 20 minute deprotection times. Coupling was executed using four fold equivalents of standard Fmoc protected amino acids (1 mmol, Chem Impex) and stoichiometric equivalents of diisopropylethylamine (DIEA, 1 mmol, Sigma Aldrich) and O-Benzotriazole-N,N,N',N'-tetramethyl-uronium-hexafluoro-phosphate (HBTU, 1mmol, Chem Impex) in DMF with a 90 minute coupling time. Palmitic acid (2 mmol) was double coupled (subsequent 90 minute coupling reactions) to the N-terminus of the peptide using DIEA (2 mmol) and HBTU (2 mmol). Upon completion of the synthesis, the peptide side chains were deprotected and the crude peptide removed from the peptidyl resin with a standard trifluoroacetic acid solution (10 mL, 95% TFA, 2.5% triisopropylsilane, 2.5% water) in a fritted peptide reaction vessel for 3 h (Chemglass Inc.). The resulting solution was filtered into a 20 mL glass vial. The crude peptide was precipitated out of solution via dropwise addition of the TFA

solution into cold diethyl ether (90 mL). The suspension in diethyl ether was transferred into two centrifuge tubes. The precipitate was pelleted using a centrifuge. The off-white to white precipitate was washed thrice with cold-diethyl ether yielding the crude material.

All peptides were purified using an Agilent Technologies HPLC Workstation equipped with a c18 column (Jupiter Proteo 10x250 mm, Phenomenex). A modified linear purification method was employed using a polar mobile phase water (0.1% TFA) with a 1% (v/v) per minute increase of the non-polar mobile phase acetonitrile (0.1% TFA). The sample was prepared at a concentration of 10 mg/mL in water (0.1% TFA) with injection volumes of 0.9 mL. The sample eluted between 50 and 60% acetonitrile (0.1% TFA). The purified peptide was isolated by removing acetonitrile via rotary evaporation. The resulting aqueous fraction was lyophilized to yield the pure peptide material as a white powder.

The purified peptides were analyzed by matrix assisted laser desorption ionization – time of flight mass spectrometry (MALDI-TOF, Bruker UltrafleXtreme) to confirm the mass of the synthesized peptides. Samples (1 μ L) were co-crystallized with 1 μ L of an α -cyano-4-hydroxycinnamic acid solution (10 mg/mL in 1:1 water/acetonitrile (0.1% TFA)) on a stainless steel MALDI plate. Calculated molecular mass were compared to experimental mass to confirm the identity of the peptide.

Molecular characterization – peptide assembly: In order to analyze secondary structure formation in the absence of (PPIX)Zn, circular dichroism spectroscopy (Jasco, Inc. J-815) was employed to analyze the typical n - π^* transitions found for a β -sheet assembly. Assembled stock solutions were prepared by adding the peptide stock solution into 30 mM NH_4OH , pH 11 solutions to yield a 1 mM stock solution. The samples were heated to 70 $^\circ\text{C}$ and then cooled. These stock solutions were then diluted into water, 10 μ L into 190 μ L to afford a 100 μ M

solution. The samples were transferred to a 1 mm quartz cuvette (Starna Cells, Inc.) and analyzed by scanning from 260 – 190 nm.

Additional secondary structural characterization was achieved with infrared spectroscopy (Thermo Scientific, Nicolet 6700 FT-IR spectrophotometer). 10 μL of the 1 mM samples described in the previous section were dropcast onto a 32 mm CaF_2 plate (Sigma Aldrich) and were air dried. The thin films were aligned in the spectrophotometer and the amide I vibrations in the region from 1500 – 1800 cm^{-1} were analyzed.

Morphological characterization: Scanning (transmission) electron micrographs were obtained with a JEOL 7500 field emission scanning electron microscope equipped with a transmission electron detector. Samples containing 100 μM of peptide were drop cast onto a 400 mesh copper grid with a carbon support film (Ted Pella). After 1 minute, the excess solution was wicked away and the sample dried.

Supplemental Results

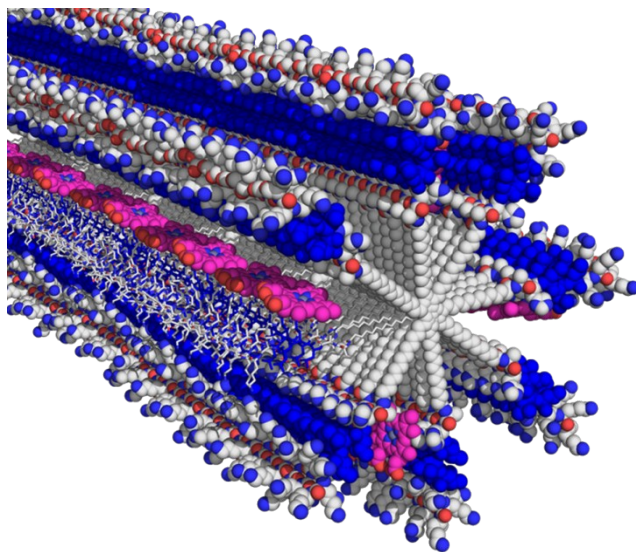


Figure S1. Illustration of the proposed supramolecular assembly of c16-AHL₃K₃-CO₂H. The fiber diameter is 7-9 nm and the (PPIX)Zn molecules are oriented along the axis of the fiber.

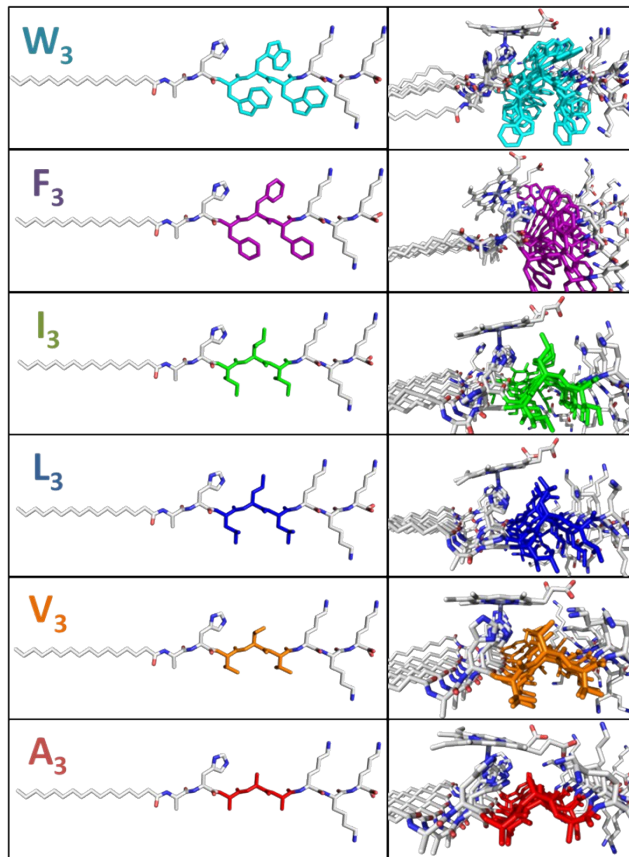


Figure S2. In c16-AHX₃K₃-CO₂H we varied the rotamers of H and X to highlight a similar impact upon cofactor interactions with respect to the amino acid side chain volume.

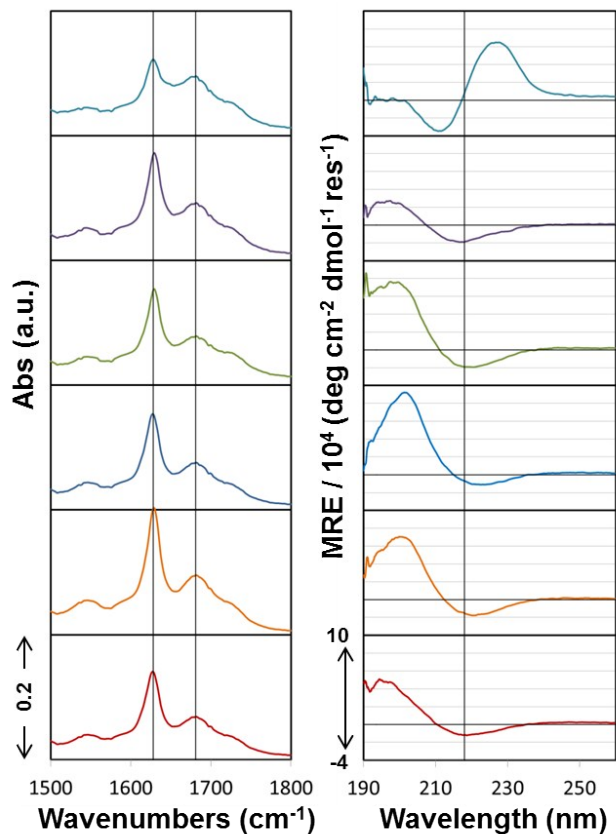


Figure S3. Secondary structural studies of the c16-AHX₃K₃-CO₂H. FTIR spectra (left) with vertical lines indicating the characteristic β -sheet amide I frequencies ($\nu = 1627$ and 1681 cm^{-1}). Circular dichroism spectra (right) with vertical line indicating the characteristic β -sheet transition ($\lambda = 218$ nm). A₃ (red), V₃ (orange), L₃ (blue), I₃ (green), F₃ (purple), W₃ (cyan).

Equation S1. The equation employed for stoichiometry and binding constant analysis is modified from a 1:1 binding model. The value 'n' is introduced here and represents the stoichiometry of peptide to heme. A_0 , initial absorption; ϵ_B , extinction of bound heme; ϵ_s , extinction coefficient contribution from scattering; x , ratio of peptide to heme; n , stoichiometry of peptide to heme; K_d , dissociation (binding) constant M , molar concentration of heme; l , cuvette pathlength.

$$A = A_0 + \frac{\epsilon_B l}{2} \times \left(\left(\frac{x}{n} \times M + K_D + M \right) - \sqrt{\left(\frac{x}{n} \times M + K_D + M \right)^2 - 4 \times \frac{x}{n} \times M^2} \right) - \epsilon_s \times l \times M + \frac{\epsilon_s l}{2} \times \left(\left(\frac{x}{n} \times M + K_D + M \right) - \sqrt{\left(\frac{x}{n} \times M + K_D + M \right)^2 - 4 \times \frac{x}{n} \times M^2} \right)$$

Sequence	Cofactor	Ref
LQEHQQA-L	FeDPP	29
IQQHTQL-A	PZn-et-Ru(tpy)	22
LQKHQQA-F	FeDPP	28
VQRHRQL-A	PZn-Ph-NDI	23
IQKHRQL-F	Zn-CF3	24
LEEHRQA-L	FeDPP	27
LQKHQQA-L	ZnDPP	30
LKLHEER-L	Heme	25
KQEHEDA-L	P*Zn	31
WKQHEEA-L	Heme	26
LKLHEER-L	Heme	26
GILHFIL-W	Heme	26
AMVLLLF-F	Heme	26
AMVLLLF-L	Heme	26

* Various porphyrin macrocycle were employed in this work

Table S1. Collected sequences indicating a predominance of Leucine at the “A”-position of the heptad. Various cofactors were used for these studies. Reference numbers correspond to those found in the main text.

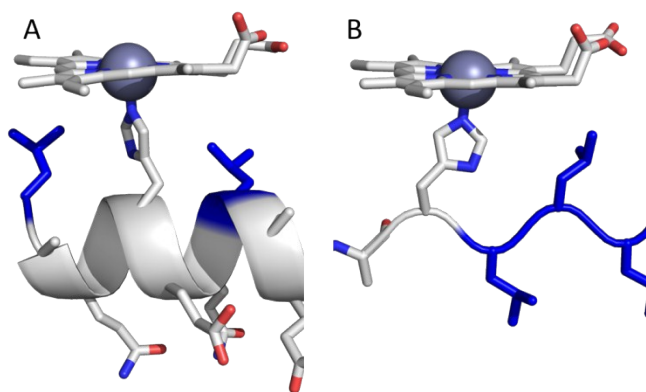


Figure S4. Stick/cartoon representations of porphyrin binding sites of (A) the β -sheet forming peptide c16-AHL₃K₃-CO₂H and (B) a helical bundle (segment – LQKHQQA). The leucine residues are colored blue to highlight their proximity to the coordinating histidine amino acid.

Figure S5. Fluorescence spectroscopic titration experiments in which 5 μM aliquots of peptide were added to a 5 μM solution of (PPIX)Zn in 30 mM NH_4OH . Excitation wavelength $\lambda = 419$ nm which is the isosbestic point in the Soret region of the UV/vis measurements. The arrows indicate the direction of intensity change upon the addition of peptide aliquots. The data points in the emission intensity vs. [Peptide]:[(PPIX)Zn] ratio represent the emission intensities at 590 nm (circles) and 650 nm (squares).

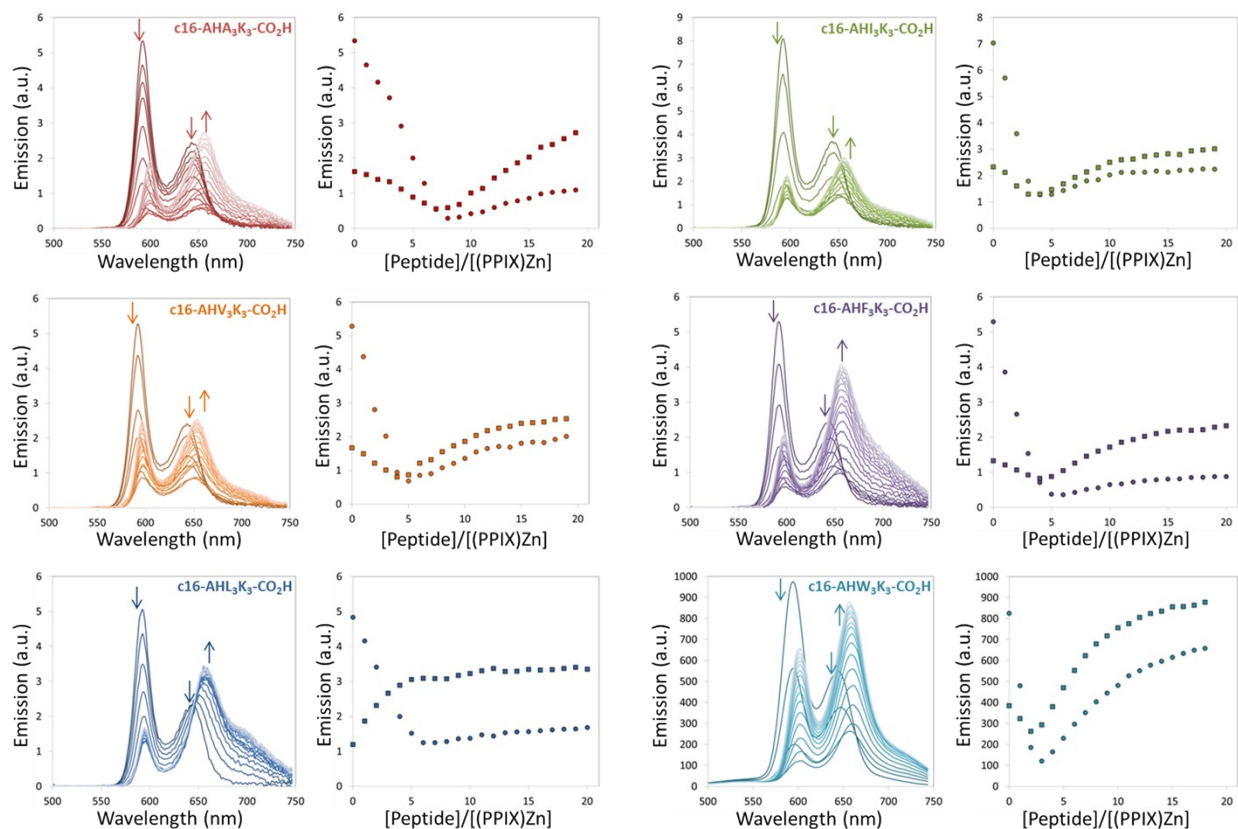


Figure S6. Picosecond transient absorption spectroscopy: A. difference spectra recorded at 100 ps delay times and B. kinetics from $\lambda = 515$ nm indicating diminished intersystem crossing as indicated by the residual triplet (T) absorption indicated as a percentage of the initial change in absorption. Note: The bleach at 650 nm is due to the emission of the excimer complex and is not observed in ZnPPIX alone.

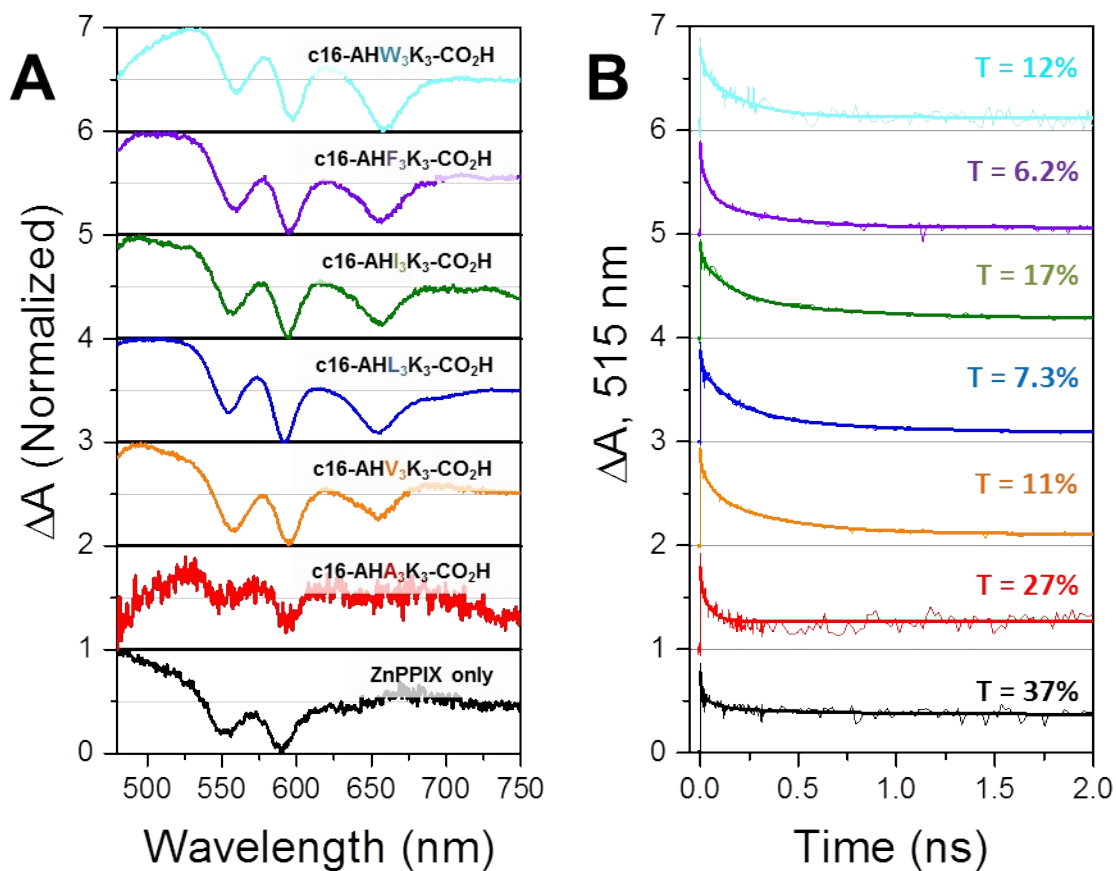
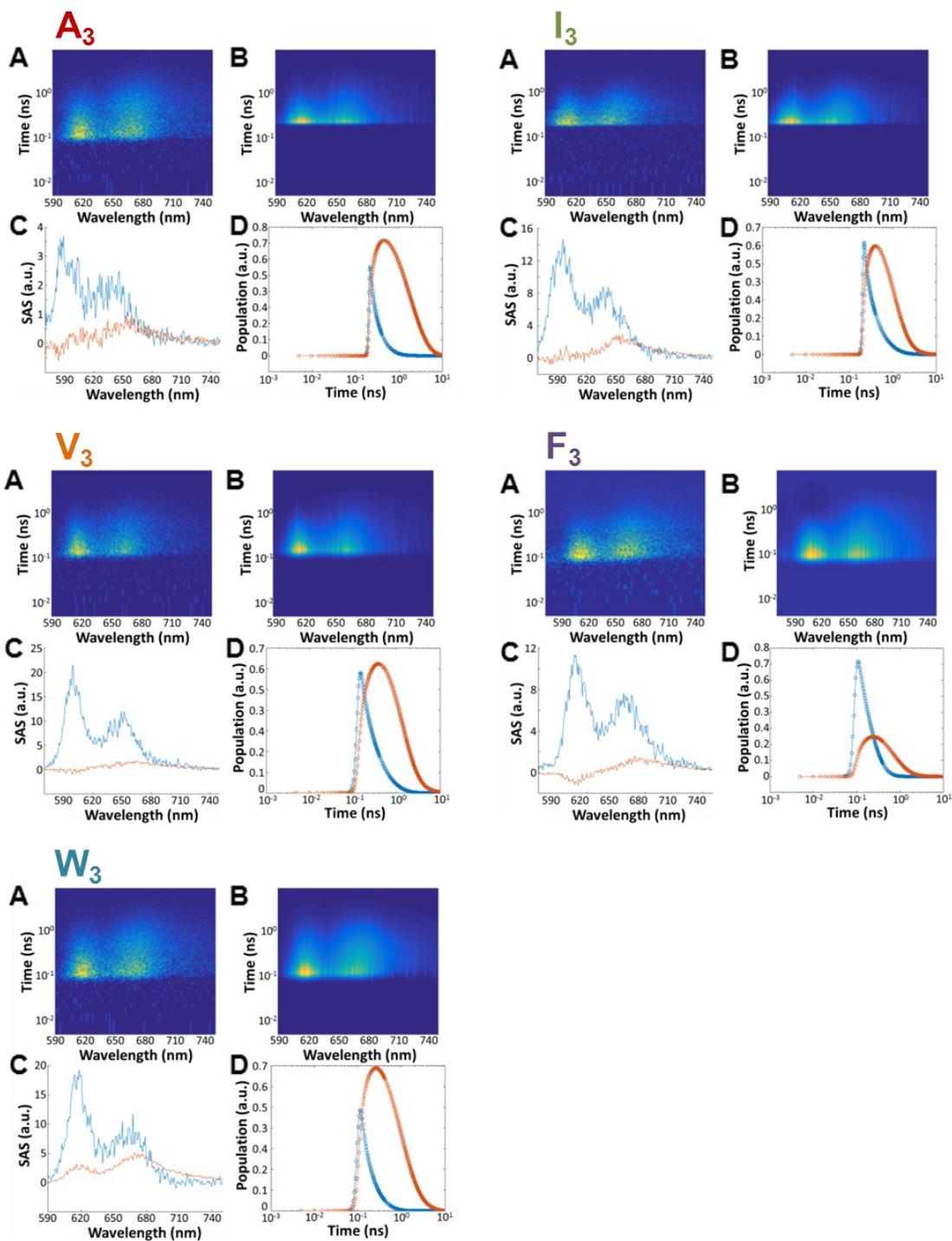


Figure S7. Global Analysis Results for determination of one dimensional exciton diffusion. Each panel represents (A) the raw data, (B) the fitted data, (C) the species association spectra, and (D) the population distribution kinetics.



Equations used in solving diffusion length (L_D) from ref 14.

Our two rates are defined by the monomer/singlet,

$$\frac{d[M_1]}{dt} = -k_a[M_0][M_1] - k_M[M_1] \quad (S1a)$$

And the excimer.

$$\frac{d[E_1]}{dt} = k_a[M_0][M_1] - k_E[E_1] \quad (S1b)$$

k_M (ns^{-1}) is the monomer decay rate constant

k_a ($\text{nm}^3 \text{ns}^{-1}$) is the association rate constant for excimer formation

k_E (ns^{-1}) is the excimer decay constant

$[M_0]$ is the monomer ground state

$[M_1]$ is the monomer excited state (the singlet)

The association rate constant in a fiber can be defined as:

$$k_a = 4\pi DR \quad (S2)$$

D is the diffusivity

R is the capture radius (1.5 nm)

In a 1D Diffusion model, k_a is time-dependent yielding k_{a0} ($\text{nm}^3 \text{ns}^{-0.5}$):

$$k_a(t) = \frac{2\pi DR^2}{\sqrt{\pi Dt}} = \frac{k_{a0}}{\sqrt{t}} \quad (S3)$$

Targeted analysis of the PL data was performed in Matlab using a nonlinear least-squares fitting algorithm using k_{a0} , k_M , and k_E as the only fitting parameters (Table S1).

D is determined using Equation S3.

1D exciton diffusion is determined with the following equation:

$$L_D = \sqrt{2D\tau_M} \quad (S4)$$

Peptide	k_M (ns^{-1})	k_E (ns^{-1})	k_{a0} ($\text{nm}^3 \text{ns}^{-0.5}$)	D ($\text{nm}^2 \text{ns}^{-1}$)	L_d (nm)
A ₃	0.35	0.24	32.9	17.1	9.9
V ₃	0.61	0.36	28.9	13.1	6.5
L ₃ *	0.60	1.08	28.3	12.6	6.5
I ₃	0.75	0.54	42.8	28.8	8.8
F ₃	1.05	0.45	49.2	38.1	8.5
W ₃	0.47	0.59	21.0	6.94	5.4

Table S2. The table summarizes the fully analyzed results. k_M , k_E , and k_{a0} are experimentally determined rate constants. D is the diffusivity along the 1D nanofiber and is determined from

k_{ao} . L_D is the diffusion length and is determined from D and k_M . For a more detailed explanation of our analytical methods see ref. 14.

References

1. Kong J & Yu S (2007) Fourier transform infrared spectroscopic analysis of protein secondary structures. *Acta Biochimica Et Biophysica Sinica* 39(8):549-559.
2. Kelly SM, Jess TJ, & Price NC (2005) How to study proteins by circular dichroism. *Biochimica Et Biophysica Acta-Proteins and Proteomics* 1751(2):119-139.